Innovative Food Science and Emerging Technologies 69 (2021) 102667

Contents lists available at ScienceDirect

Innovative Food Science and Emerging Technologies

journal homepage: www.elsevier.com/locate/ifset

Effects of layer arrangement on heating uniformity and product quality after hot air assisted radio frequency drying of carrot

Chenchen Wang [a], Xiaoxi Kou [a], Xu Zhou [b], Rui Li [a], Shaojin Wang [a,b,*]

[a] College of Mechanical and Electronic Engineering, Northwest A&F University, Yangling, Shaanxi 712100, China
[b] Department of Biological Systems Engineering, Washington State University, 213 L.J. Smith Hall, Pullman, WA 99164-6120, USA

ARTICLE INFO

Keywords:
Carrot slices
Heating uniformity
Radio frequency
Combined drying
Quality

ABSTRACT

The conventional drying technology prolongs the shelf life of carrots but may cause the serious loss of nutrients. The aim of this study was to investigate the effects of intermittently rearranging layers on the heating uniformity, drying characteristics and quality of carrot slices under the hot air assisted radio frequency (RF) heating. The carrot slices were dried for 270 min using hot air (60 °C) assisted RF heating at the electrode gap of 100 mm firstly, and then followed hot air drying to achieve the final moisture level (0.11 kg/kg (d.b.)). The results showed that the selected hot air assisted RF drying protocol for the carrot slices reduced 30% of the duration compared to the single hot air drying. The carrot slices dried by the combined drying method had the highest total carotenoid value ($P \leq 0.05$) except for possessing accepted color and rehydration. Therefore, the combined drying method could improve the drying rate and maintain heat sensitive substances in carrot slices.

1. Introduction

Carrot (*Daucus carota L.*) is one of the most widely cultivated vegetables with rich nutrient compositions, such as vitamin A and β-carotene (Chen, Guo, & Wu, 2016; Lau, Van Chuyen, & Vuong, 2018; Zhang et al., 2018). The production and consumption of carrot are steadily increasing. Especially, China had the largest carrot production (18.02 Mt) in the world in 2018 (FAOSTAT, 2018). However, the initial moisture of fresh carrot is too high for long-term stable storage. Dehydration technology is an efficient method to prolong shelf life and improve transportation convenience of carrots (Sutar & Prasad, 2007).

The conventional dehydration treatments include hot air drying (Mbondo, Owino, Ambuko, & Sila, 2018). Hot air drying is a common and convenient technology that applied in many kinds of vegetable and fruit, such as kiwifruit (Guine, Brito, & Ribeiro, 2017; Maskan, 2001), eggplant (Doymaz & Aktas, 2018; Guine et al., 2017), and pumpkin (Ando, Okunishi, & Okadome, 2019). However, the products dried by hot air have many drawbacks, such as the color degradation and the low residual ratio of the heat-sensitive antioxidant active substances due to the long drying duration (Goula & Adamopoulos, 2010). Therefore, to avoid product quality degradations caused by traditional drying methods, dielectric heating-related technologies have been introduced as new drying processes (Zhou & Wang, 2018).

Many studies have been conducted on the dielectric heating in food processing (Jiao, Tang, Wang, & Koral, 2018; Zhang, Tang, Mujumdar, & Wang, 2006). The mechanism of dielectric heating is to transfer electric energy to thermal one volumetrically by molecular polarization and ionic conductance. Dielectric processing includes microwave heating and radio frequency (RF) heating. The microwave technology has been applied in many areas, such as blanching (Sezer & Demirdoven, 2015), drying (Cui, Xu, & Sun, 2004; Cui, Xu, Sun, & Chen, 2005), and sterilization (Wang, Wig, Tang, & Hallberg, 2003). Since the wavelength of an electromagnetic wave is inversely proportional to its frequency (Wang et al., 2001), RF energy has the advantage of large penetration depth for applying to industry-scale food processing, especially in postharvest disinfestation (Hou, Liu, & Wang, 2019; Ling, Cheng, & Wang, 2020; Wang, Monzon, Johnson, Mitcham, & Tang, 2007), thawing (Li et al., 2018), pasteurization (Li, Kou, Cheng, Zheng, & Wang, 2017; Li, Kou, Hou, Ling, & Wang, 2018), and drying (Zhou & Wang, 2018). In general, RF drying has been applied for walnuts (Zhang, Zheng, Zhou, Huang, & Wang, 2016; Zhou, Gao, Mitcham, & Wang, 2017), kiwifruits (Zhou, Ramaswamy, Qu, Xu, & Wang, 2019), macadamia nuts (Wang et al., 2014), and mango slices (Zhang et al., 2019) to improve drying efficiency and quality of products. Besides, the heating characteristics and direction of mass transfer in the RF field can produce a puffing effect on dried crisps of some products (Roknul, Zhang,

* Corresponding author at: College of Mechanical and Electronic Engineering, Northwest A&F University, Yangling, Shaanxi 712100, China.
E-mail address: shaojinwang@nwsuaf.edu.cn (S. Wang).

https://doi.org/10.1016/j.ifset.2021.102667
Received 9 September 2020; Received in revised form 11 March 2021; Accepted 15 March 2021
Available online 18 March 2021

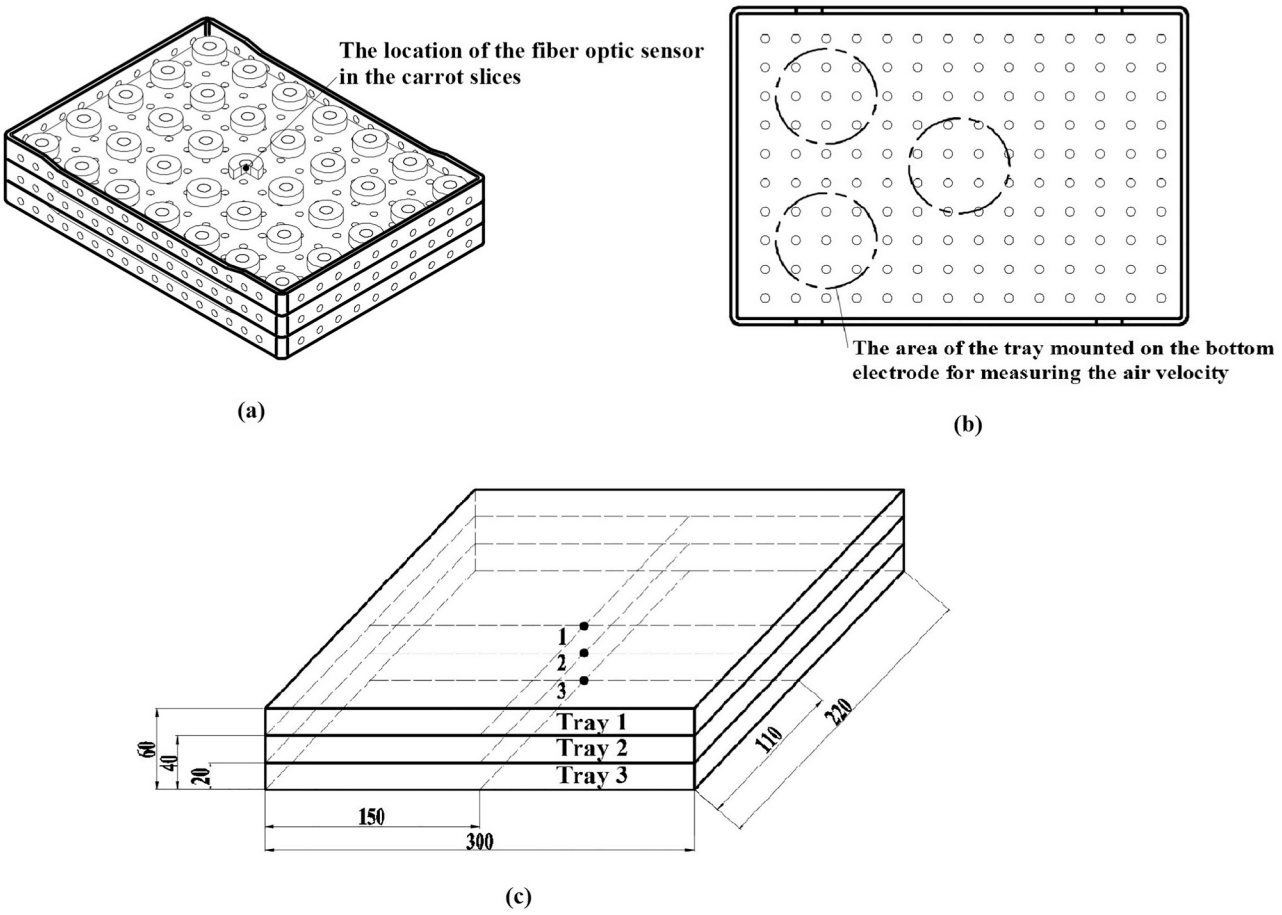

Fig. 1. Location distributions of the carrot slices (a) and three fiber optic sensors (1–3)(b) and the area of tray for measuring the air velocity (all dimensions are in mm).

Mujumdar, & Wang, 2014).

Improving the residual content of heat-sensitive nutrients in dried products without compromising with duration has been focused in Zhou and Wang (2018). Although RF energy has great potential to rapidly heat samples, the bending characteristics of the RF field around the corner and edge of the containers result in the uneven temperature distribution in the material (Huang, Zhang, Marra, & Wang, 2016). Besides, the degradation of heat-sensitive nutrient content in carrots, such as carotenoid, caused by long duration in hot air drying process is a critical issue (Goula & Adamopoulos, 2010). Combined hot air with RF drying is a promising drying method to take advantages of both technologies (Zhou et al., 2019). Although RF energy has shown the advantage of improving the drying rate and content of vitamin C simultaneously for some products (Zhang et al., 2019), a systematic study on implementation of RF energy in drying processing for carrot slices with high content of carotenoid is still needed.

The specific objectives of this study were to (1) analyze the effect of electrode gaps on hot air assisted RF drying characteristics of the carrot slices in multiple layers, (2) study the effect of rearranging layers at different time intervals on heating and drying uniformity of multi-layer slices during hot air assisted RF drying, (3) determine the parameters of the combined drying protocol for the slices in multiple layers, and (4) compare the product quality of the dried slices between the selected combined drying and individual hot air drying methods.

2. Materials and methods

2.1. Sample preparation

Fresh carrots (*Daucus carota* L. cultivar "Guanghong") were purchased from the local market at Yangling, Shaanxi, China. Samples were stored in a refrigerator at 4 °C. Before experiments, the samples were taken out and equilibrated in an incubator (GD/JS4010, Haixiang Instrument & Equipment Co., Ltd., Shanghai, China) at 25 ± 0.5 °C for 10 h. The samples were cut into round slices with diameter of 34 ± 0.50 mm by using a corer into a cylinder (with the axis along the direction of the root growth) and thickness of 7.92 ± 0.27 mm, which was selected for obtaining suitable heating rate by taking advantage of deep penetration in the RF field and high content of total carotenoid of production (Alam, Lyng, Frontuto, Marra, & Cinquanta, 2018; Goula & Adamopoulos, 2010; Zhou et al., 2018). All experiments were performed with three trays of samples, and thirty-five freshly prepared carrot slices (total weight of 242.48 ± 2.37 g) were spread uniformly in a single layer inside each tray (400 mm *L* × 270 mm *W* × 20 mm *H*) (Fig. 1a). The tray was made of poly-propylene perforated with 10 mm diameter holes along its side and bottom walls. To avoid high-localized temperature at contact points among samples, each slice was separated from adjacent ones (Hou, Huang, Kou, & Wang, 2016).

The initial moisture of fresh carrot was 9.90 ± 0.91 kg [water]/kg [solid] in dry basis (d.b.). The moisture determination followed the oven method as described in Zhou et al. (2018).

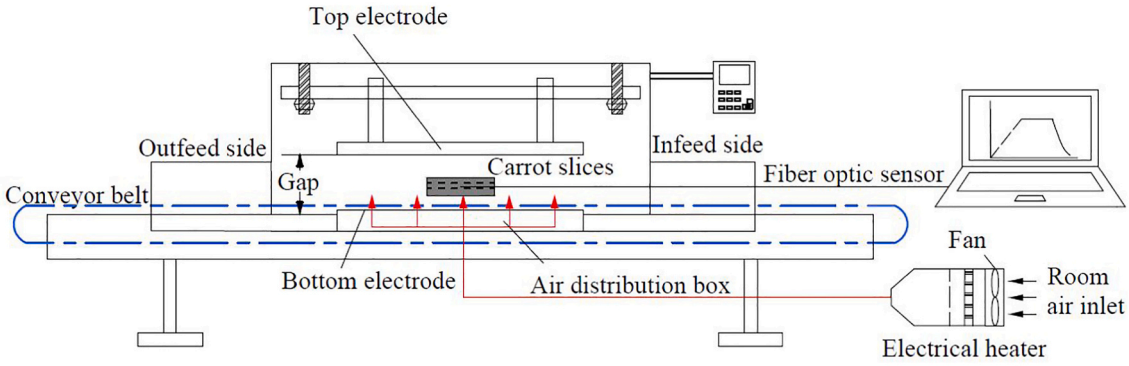

Fig. 2. Schematic view of the pilot-scale 6 kW, 27.12 MHz RF system (Adapted from Wang et al., 2010).

2.2. Drying experiments

2.2.1. Determining the suitable electrode gap

A 6 kW, 27.12 MHz pilot-scale free running oscillator RF system (SO6B, Strayfield International, Wokingham, UK) combined with a hot-air system supplied by a 6 kW electric heater was used for hot air assisted RF drying experiments (Fig. 2). The detailed description of the RF unit and hot-air heating system can be found in Wang, Tiwari, Jiao, Johnson, and Tang (2010).

To obtain a suitable electrode gap for drying carrot slices, three trays of samples, prepared as illustrated in Fig. 1a, were used in this part of experiments. Before experiments started, three trays with samples were stacked vertically together and placed on the central area of the bottom electrode. Three levels of electrode gap (90, 100 and 110 mm) were selected to study the drying and heating characteristics of carrot slices in hot air assisted RF drying (Zhang et al., 2016). The temperature and velocity of hot air heating system were 60 °C and about 1.0 m/s, respectively, which were measured by fiber-optic temperature sensors (HQ-FTS-D120, Heqi Technologies Inc., Xian, China) and an anemometer (DT-8880, China Everbest Machinery Industry Co., Ltd., Shenzhen, China) (Fig. 1b). The temperature and velocity of hot air were selected by saving the content of total carotenoid in dried production and shortening treatment duration (Alam et al., 2018; Goula & Adamopoulos, 2010).

The hot air heating system was started for warming up about 45 m before the drying process, until the environment in the RF cavity was reaching the steady temperature condition. Five fiber-optic temperature sensors were fixed at the corners and the center of the tray located on the bottom electrode to monitor the sample temperature. Three fiber-optic temperature sensors were mounted in the geometric center of the carrot slices on the central point in each tray to monitor the slices located on the "cold spots" of each tray in RF heating (Fig. 1c) (Huang et al., 2016). This part of experiments continued for 210 min (Lau et al., 2018). To avoid quality deterioration of carrot slices in high temperature environment and maintain the equipment safety, this test ceased when the maximum temperature of the sample exceeded 80 °C. To record the moisture content data of samples in each tray during drying experiments, the container was removed from RF heating system through the infeed side every hour for determining the weight of the sample by using an electric balance (PTX-FA210, Huazhi Scientific Instrument, Co., LTd., Fuzhou, China) with a precision of 0.01 g. The total measurement duration was less than 30 s. The initial and final surface temperatures of every slice were recorded by infrared camera (FLIR A300, FLIR Systems AB, Stockholm, Sweden) for evaluating the heating uniformity of samples in each tray dried by different treatment methods, and the data of temperature images were used to analyze the heating uniformity (Wang et al., 2007).

The uniformity index (λ) of samples was used to evaluate the RF heating uniformity of samples in the drying experiments (Wang et al., 2007):

$$\lambda = \frac{\Delta\sigma}{\Delta\mu} \tag{1}$$

where $\Delta\sigma$ is the rise (°C) in the standard deviation of product temperature and $\Delta\mu$ is the rise (°C) in mean product temperature over the treatment time. The smaller λ values stand for better heating uniformity.

2.2.2. Determining the proper interval of drying time to rearrange the tray layers

For improving drying and heating uniformity of the carrot slices among each tray, rearranging layers was applied during hot air assisted RF drying. The specific details of rearranging layers to implement in a reciprocating cycle were as follows: the rearranging order of three single trays in the vertical direction was based on the study of "Drying experiment 1", by firstly moving trays from tray 1, tray 2 and tray 3 to tray 3, tray 1 and tray 2. After the samples in each tray were dried for a certain period (15, 30 and 60 min), moving from tray 3, tray 1 and tray 2 to tray 2, tray 3 and tray 1, and finally moving trays from tray 2, tray 1 and tray 3 to tray 1, tray 2 and tray 3 were performed as shown in Fig. 3. The maximum drying time was 420 min to avoid the quality deterioration of samples caused by overheating. At each stage of rearranging layers, the sample surface temperature and weight were obtained. The durations of rearranging layers and weighing were less than 10 and 45 s to reduce the heat loss. The moisture content and uniformity index (λ) were determined as mentioned above.

2.2.3. Hot air drying and selecting the appropriate combined drying protocol

Hot air drying (HAD) for carrot slices was accomplished through a cross-flow tray drier (DHG-9030A, Precision & Scientific Instrument Co. Ltd., Shanghai, China) with an air speed of 1.0 m/s as measured by the anemometer described above, and temperature of 60 °C, which were selected as same as hot air heating system in RF equipment. Before the experiments were started, the tray dryer was preheated for 30 min to obtain the steady temperature conditions, and samples in polypropylene (PP) containers were fixed on the central area of the dryer cavity. The measurement of sample moisture contents in each layer was conducted at each hour until the average moisture content of samples in each tray reached at the target moisture level, which was less than 0.11 kg/kg in dry basis (d.b.) (Cui et al., 2004; Xu et al., 2018). The dried samples were used for evaluation of product quality.

To avoid the overheating in the final stage of hot air assisted RF drying for carrot slices, the combined drying was recommended as an effective method to take advantages of both drying technologies. Thus, samples were dried by hot air assisted RF heating with rearranging

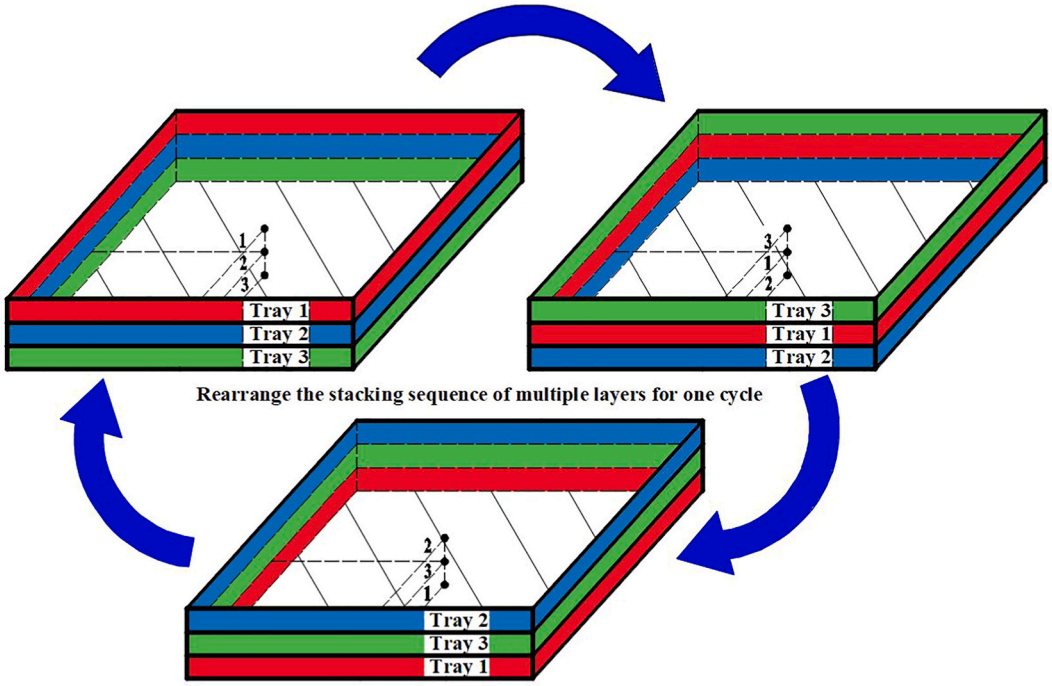

Fig. 3. Schematic diagram for rearranging the stacking sequence of multiple layers in a container.

layers for different numbers of reciprocating cycle. Since the duration of a cycle was 90 min, carrot slices were processed by the hot air assisted RF system for 270, 360 and 450 min, respectively, which were expressed as combined point 1, combined point 2 and combined point 3. Then the RF with hot air heating system was turned off, and the samples in three trays were transferred into the hot air drier immediately, and the remaining moisture content of samples was dried by hot air drying until the average moisture content of samples in each tray arrived at the target moisture level (Fig. 4). The different combined drying protocols were expressed as Comb-D 1, Comb-D 2 and Comb-D 3, which were based on the different duration for slices processed in RF cavity. The moisture content of samples was measured as described above, and the infrared imaging of samples was captured at each combined point to calculate the uniformity index to study the heating characteristics and select the samples with high temperatures and uneven heating for comparing the product quality dried by different methods.

2.2.4. Calculation of drying rate and effective diffusivity coefficient

$$\mathrm{DR} = \frac{M_{t_1} - M_{t_2}}{t_2 - t_1} \tag{2}$$

The drying rate (*DR*) of carrot slices during drying experiments was computed using Eq. (2) and expressed as kg water/ kg solid min^{-1}:

Where t_1 and t_2 are the drying times (min) during drying, M_{t1} and M_{t2} are the moisture contents on a dry basis of carrot slices at time t_1 and t_2, respectively.

To evaluate the moisture transfer mechanisms of drying experiments, the effective diffusivity coefficient (D_{eff}) was introduced in this study and calculated according to Zhou et al. (2018). Based on the assumptions of neglecting shrinkage, uniform initial sample moisture content distribution, and constant heat/mass transfer, the diffusion solution of the Fick's second law can be given below for various sample geometrics during the falling drying rate period (Crank, 1975):

$$\mathrm{MR} = \frac{M_i - M_e}{M_o - M_e} = \frac{8}{\pi^2}\sum_{n=0}^{\infty}\frac{1}{(2n+1)^2}exp\left(\frac{-(2n+1)^2\pi^2 D_{eff}t}{4(h)^2}\right) \tag{3}$$

where the carrot slices were considered as the homogeneous slab, *MR* is the dimensionless moisture ratio, M_i is the moisture content (kg/kg, d.b.) at any time *i*, M_0 is the initial moisture content (kg/kg, d.b.) and *Me* is the equilibrium moisture content (kg/kg, d.b.), D_{eff} is the effective diffusivity coefficient (m^2/s), *h* is the half thickness of the slab (m), and *n* is a positive integer. In long period drying experiments, Eq. (3) could be simplified in practice when the first term of series solution is applied (Crank, 1975):

$$\mathrm{MR} = \frac{M_i - M_e}{M_o - M_e} = \frac{8}{\pi^2}exp\left(\frac{-\pi^2 D_{eff}t}{4(h)^2}\right) \tag{4}$$

Eq. (4) could be transferred into the logarithmic form:

$$ln(MR) = ln\left(\frac{8}{\pi^2}\right) - \frac{\pi^2 D_{eff}t}{4(h)^2} \tag{5}$$

According to Eq. (5), the plot of ln (*MR*) versus *t* (s) would be linear, and the slope could be used to calculate the (D_{eff}).

Since the significant shrinkage of carrot slices was ignored during the drying process, the *Deff* calculated by the above method would be treated as overestimated values, but could be allowed for the parallel comparison among various drying processes.

2.3. Evaluation of product quality

2.3.1. Color analysis

The color of fresh and dried samples was measured using a computer vision system, which included a lighting system and a Canon EOS 600 Digital camera with 1800 megapixels resolution and EF-S 18–55 mm f/ 3.5–3.6 Zoom Lens interfaced to a computer. The detailed description of the computer vision system could be found in Zhou, Ling, Zheng, Zhang, and Wang (2015). To avoid the shrinkage effects of the dried samples on the accuracy of measurement, the samples were powdering before the color test. After the computer vision system warming up for 20 min to obtain the steady light condition, the sample powder was placed uniformly in a white plastic container (Diameter: 40 mm; Height: 11 mm; Thickness: 1 mm) for color determination, which was obtained from the drying experiments. The color was expressed in the CIE systems where the values of L^*, a^*, b^* presented darkness-lightness, greenness-redness,

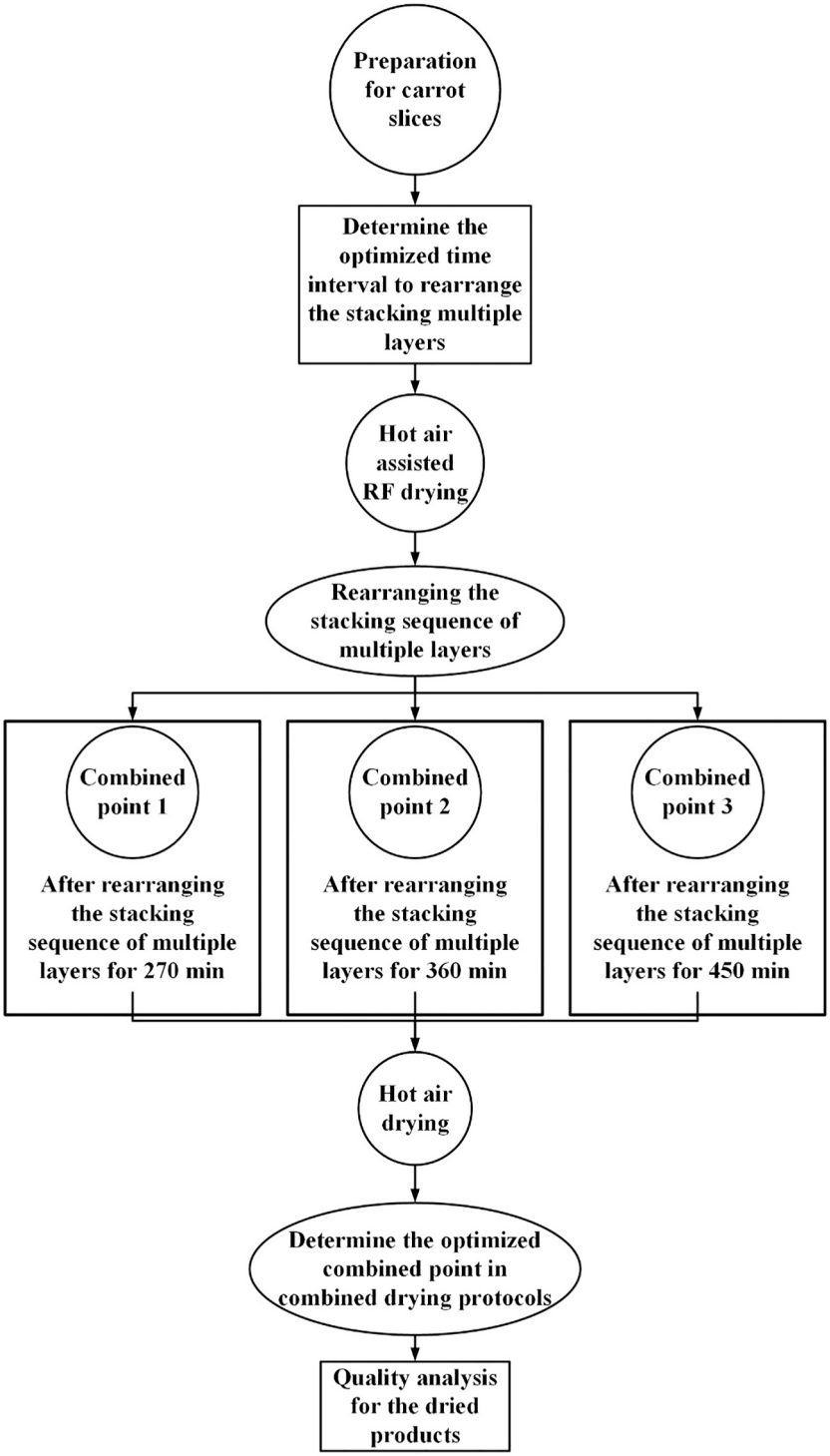

Fig. 4. Schematic flowchart to select the combined point in combined drying protocols.

and blueness-yellowness, respectively. The total value of the color difference (ΔE) was calculated as follows:

$$\Delta E = \sqrt{\left(L^* - L_0^*\right)^2 + \left(a^* - a_0^*\right)^2 + \left(b^* - b_0^*\right)^2} \quad (6)$$

where ΔE is color change, L_0* and L* are the lightness values of fresh and dried samples, respectively, a_0* and a* are the greenness-redness values of fresh and dried samples, respectively, and b_0* and b* are the blueness-yellowness values of fresh and dried samples, respectively.

2.3.2. Rehydration capacity

Rehydration capacity of dried carrot slices was measured according to the method of Zhou et al. (2018) with a little adjustment. Five dried slices were randomly selected from each tray, which was about 3–4 g, were weighed and then immersed into a beaker containing hot water (50 °C). After 15 min, rehydrated samples were taken out and drained over a filter paper for 25 s to remove the water adsorbed on the surface and then reweighed. The rehydration capacity was expressed as a percentage of weight gain from the initial weight and calculated as follows:

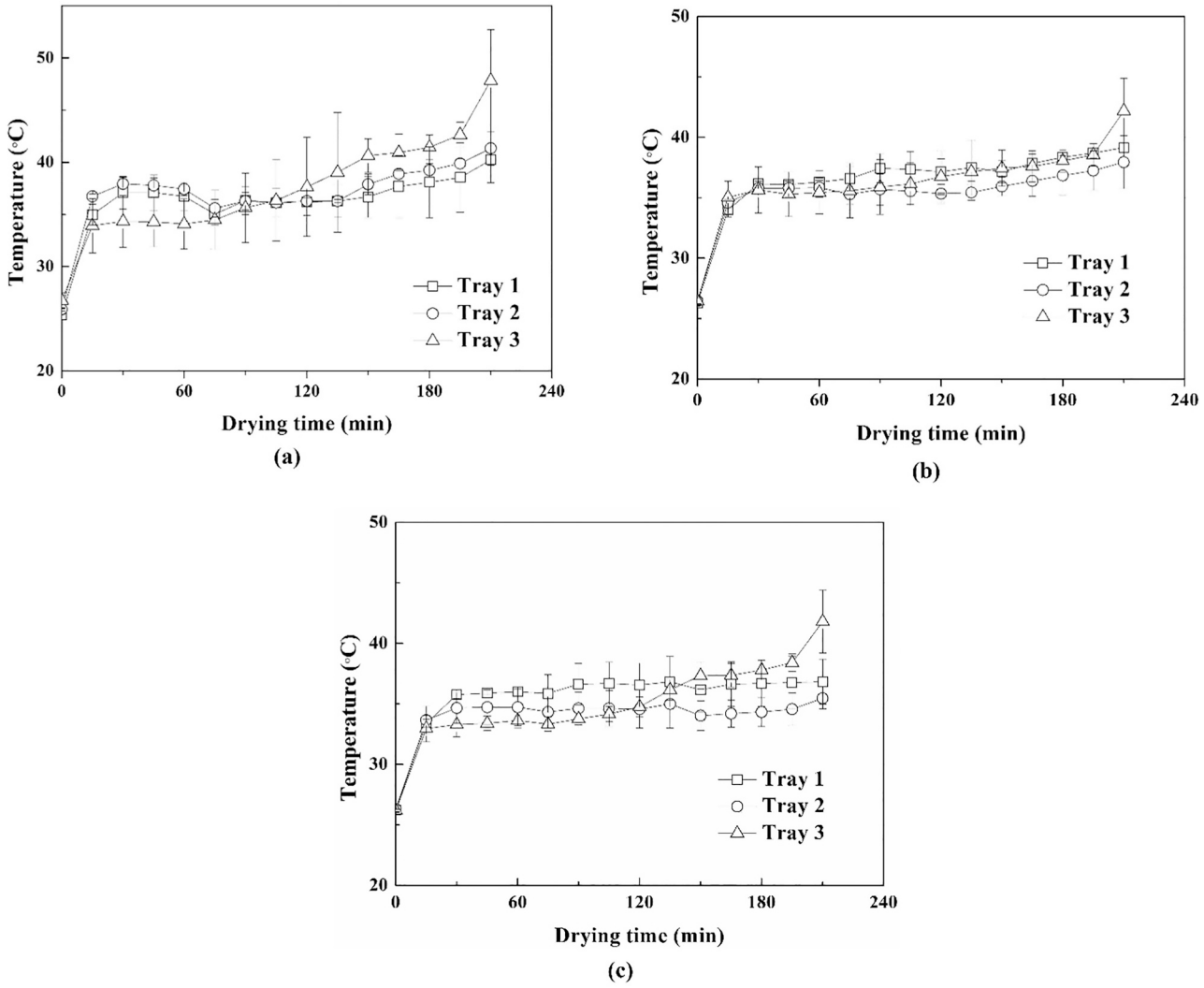

Fig. 5. Temperature-time histories of carrot slices at the locations of 1, 2 and 3 (Fig. 1) in three trays during 210 min of RF assisted hot air drying under three electrode gaps (90 mm (a), 100 mm (b) and 110 mm (c)).

$$\text{Rehydration capacity} = \frac{W - W_0}{W_0} \times 100\% \quad (7)$$

where W_0 and W are the sample weight values (g) before and after rehydration, respectively.

2.3.3. Determination of total carotenoid content

Total carotenoids were determined using the method described by Rawson, Tiwari, Tuohy, O'Donnell, and Brunton (2011) with a little adjustment. The fresh and dried carrot slices were powdering and weighed with the powder samples of 4.5 g and 0.5 g, respectively. Then the powder was mixed with 25 mL of hexane: acetone (7:3) using a homogenizer (FSH-2A, Chengdong Xinrui Instrument Company, Jintan, China) at 16,000 rpm for 5 min. The samples were thoroughly mixed with a vortex mixer (XW-80A, Haimen Kylin-Bell Lab Instruments Co. Ltd., Haimen, China) for 20 min at 2800 rpm and then centrifuged (SC-3610, Anhui Ustc Zonkia Scientific Instruments Co., Ltd., Anhui, China) for 20 min at 4000 rpm. The residue was re-extracted until it became colorless. The filtrates were combined in a separating funnel and washed with 50 mL of distilled water. The water phase was discarded and Na_2SO_4 (10 g) was added as a desiccant. The organic phase of the extract was transferred to a 50 mL beaker and hexane: acetone (7:3) added to make a 50 mL volume. The absorbance of this solution was then determined at 450 nm using a UV–Vis spectrophotometer (UV-2000, Unico Instrument Co., Ltd., Shanghai, China). External calibration with authenticated β-carotene standards solutions (0.5–10 μg/mL) in hexane: acetone (7:3) was used to quantify carotenoids in the solutions.

2.4. Statistic analysis

Test results were expressed as mean ± standard deviations of all observations from two replicates. The significance of the effects of different treatments on the uniformity index (λ), ΔE, rehydration capacity and the total carotenoid content of dried production were examined by conducting a one-way analysis of variance (ANOVA) using SPSS 17.0 (SPSS Inc., USA). All of the statistical tests were performed at a significance level of $P = 0.05$.

3. Result and discussion

3.1. Effect of electrode gaps on drying characteristics of the carrot slices in each tray

Fig. 5 shows the inner temperature evolution of the samples after hot air assisted RF drying for 210 min, showing a rise trend. The temperature of the slices in the tray 3 was the highest when using the same electrode gap, and ascended as the electrode gap decreased. Because of the bending characteristics of RF field, the inner temperature difference

Table 1
The average surface temperature and uniformity index (λ) of the carrot slices in each layer after hot air assisted RF drying for 210 min.

Electrode gap (mm)	90	100	110
Average temperature (°C)			
Tray 1	38.34 ± 2.41	35.77 ± 1.39	35.23 ± 1.20
Tray 2	40.17 ± 2.57	36.92 ± 1.61	35.53 ± 1.22
Tray 3	44.95 ± 4.40	40.16 ± 2.04	39.49 ± 1.56
Uniformity index (λ)			
Tray 1	0.070 ± 0.028Aa*	0.077 ± 0.004Aa	0.077 ± 0.016Aa
Tray 2	0.095 ± 0.005Aa	0.076 ± 0.007Aa	0.075 ± 0.027Aa
Tray 3	0.176 ± 0.043Aa	0.100 ± 0.018Ab	0.080 ± 0.008Bb

* Different lowercase and uppercase letters indicate that there is a significant difference ($P \leq 0.05$) in the heating uniformity index among the trays and electrode gaps, respectively.

of the samples in each layer was enlarged with increased RF field intensity. This phenomenon may be caused by the non-uniform distribution of the RF field in the processing. As the electrode gap decreased, the RF field was more concentrated in the bottom layer. Similar results can also be found in Hou et al. (2016). Table 1 lists the surface temperature of the samples after dried by hot air assisted RF heating for 210 min. The final surface temperature of samples was distributed as the central temperature of samples shown in Fig. 5. The same results could be observed in the process of the bulk sample heated by RF energy (Huang et al., 2016).

Fig. 6 shows the difference in drying curves of samples at different electrode gaps for 210 min, indicating that the drying rate was improved by reducing the electrode gap but with the low drying uniformity. The drying uniformity of samples dried by hot air could be attributed to the rise of relative humidity in hot air flow (Zhou et al., 2018). The high value of temperature and uniformity index (λ) in samples on the bottom layer is not only affected by the RF field distribution but also the influence of air flow direction. The heating characteristics caused by the energy consumption of samples may exacerbate the non-uniform heating in the RF field. The non-uniform heating characteristics of samples could lead to a large drying difference of samples among each tray. In the recent study of Roknul et al. (2014) and Zhou et al. (2019), arcing and sharply rising temperature of samples would be a serious problem to cause irreversible damage to the quality of slices in tray randomly, suggesting that the protocol should be stable and effective. Besides, the energy imbalance in the subsequent drying process, especially at the electrode gap of 90 mm, caused the serious loss of color attribute (ΔE and a^*) of samples dried for 210 min (Table 2). To improve the quality of the product in this study without compromising on the drying rate, the electrode gap of 100 mm was selected in further studies.

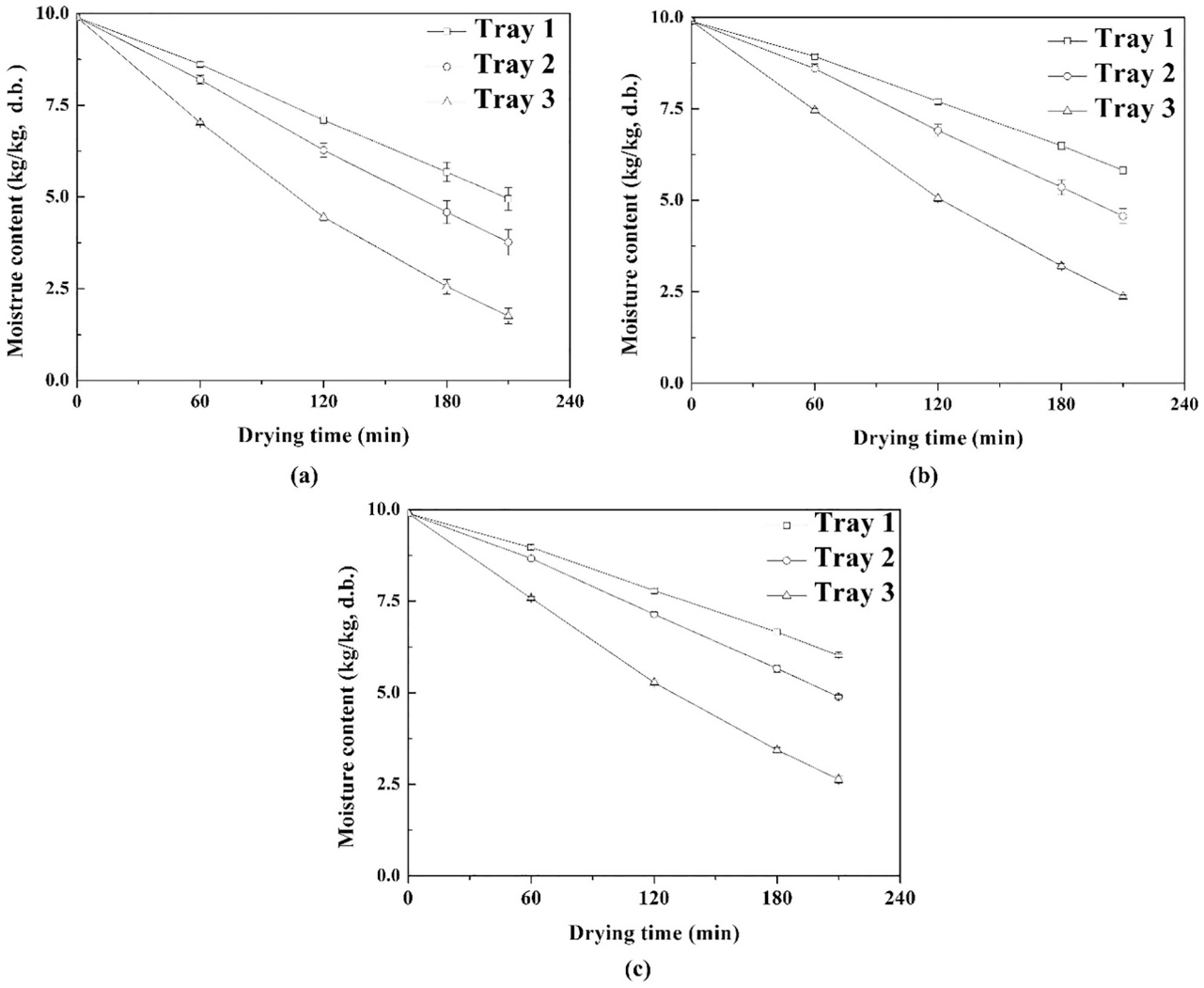

Fig. 6. Drying curves of carrot slices with RF assisted hot air heating for 210 min under three electrode gaps (90 mm (a), 100 mm (b) and 110 mm (c)).

Table 2
The color analysis of carrot slices in each tray after hot air assisted RF drying for 210 min in different electrode gaps.

	Fresh	Tray 1			Tray 2			Tray 3		
Gap	–	90 mm	100 mm	110 mm	90 mm	100 mm	110 mm	90 mm	100 mm	110 mm
L^*	36.94 ± 1.06	35.50 ± 1.63A#	35.74 ± 1.00A	36.72 ± 0.28A	35.15 ± 2.07A	37.00 ± 0.62A	35.41 ± 0.56A	34.35 ± 1.51A	37.30 ± 0.92A	35.66 ± 0.47A
a^*	40.50 ± 0.82	39.33 ± 0.50A	39.15 ± 0.21A	39.59 ± 0.47A	38.93 ± 0.99A	40.18 ± 0.20A	39.50 ± 0.58A	38.19 ± 0.30A	40.45 ± 0.07B	39.68 ± 0.15C
b^*	39.93 ± 0.27	38.38 ± 0.93A	38.23 ± 0.49A	38.74 ± 0.09A	38.20 ± 1.20A	38.87 ± 0.09A	37.86 ± 0.16A	37.12 ± 0.46A	38.96 ± 0.41B	38.16 ± 0.40AB
ΔE	–	2.49 ± 1.76A	2.53 ± 0.92A	1.54 ± 0.38A	3.00 ± 2.44A	1.21 ± 0.01A	2.81 ± 0.21A	4.51 ± 1.30A	1.26 ± 0.05B	2.34 ± 0.61AB

Different uppercase letters indicate that there is a significant difference in the color quality of the sample in the same tray among electrode gaps at $P \leq 0.05$;

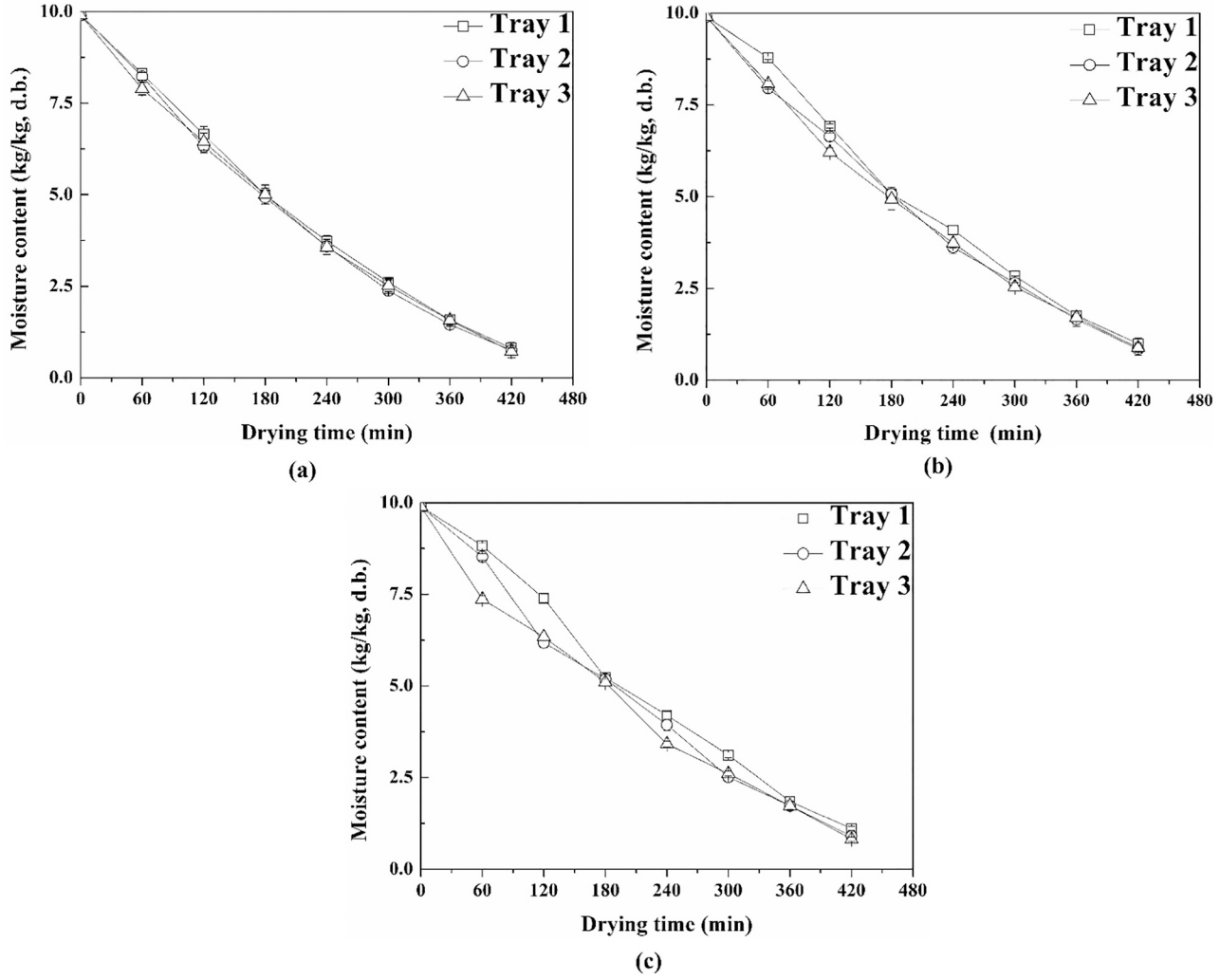

Fig. 7. Drying curves of carrot slices using RF (100 mm electrode) assisted hot air (60 °C) and rearranging layer at three-time intervals (15 min (a), 30 min (b), and 60 min (c)).

3.2. Effect of rearranging layers at different time intervals on drying characteristics of slices in each tray

Fig. 7 shows the drying curves of carrot slices after hot air assisted RF drying with rearranging layers at the time intervals of 15 min (Fig. 7a), 30 min (Fig. 7b) and 60 min (Fig. 7c). It could be observed from the drying curves that rearranging layers at lower interval time could reduce the difference among the drying curves of carrot slices in each tray, suggesting that RF energy could improve drying uniformity by rearranging layer in drying processing for multi-layer slices. This phenomenon could be attributed to the redistribution of interaction field of RF field and hot air to balance the cumulative effect on multi-layer samples.

To ensure the high ratio of heat-sensitive nutrients in products, the selected interval in hot air assisted RF drying for carrot slices to rearrange layers is bounded to compare the uniformity index (λ) and drying curves of samples with different treatments. The uniformity index (λ) values indicated that the selected interval of time in drying process was 30 min (Table 3). The results showed that rearranging layers at interval of 60 min caused the low surface temperature and poor heating uniformity of slices in tray 1, and rearranging layers at interval of 15 min caused a rise trend both in surface temperature and heating uniformity of multi-layer samples.

To keep the balance of drying rate and heating uniformity, rearranging layers at the time interval of 30 min was selected in further

Table 3
The average surface temperature and uniformity index (λ) of the slices in each tray after hot air assisted RF drying for 420 min with rearranging layers at different intervals of time.

Time interval (min)	15	30	60
Average temperature (°C)			
Tray 1	51.50 ± 3.53	48.82 ± 3.45	46.58 ± 2.24
Tray 2	52.91 ± 3.20	51.41 ± 3.51	48.77 ± 1.28
Tray 3	50.45 ± 2.09	48.96 ± 2.81	49.77 ± 1.39
Uniformity index (λ)			
Tray 1	0.171 ± 0.001Aa*	0.186 ± 0.012Aa	0.214 ± 0.005Ba
Tray 2	0.176 ± 0.014Aa	0.171 ± 0.019Aa	0.176 ± 0.039Aa
Tray 3	0.192 ± 0.074Aa	0.159 ± 0.008Aa	0.152 ± 0.016Aa

* Different lowercase and uppercase letters indicate that there is a significant difference ($P \leq 0.05$) in the heating uniformity index among trays and time intervals, respectively.

studies.

3.3. Drying characteristics of carrot slices on each layer dried by individual hot air and different combined drying protocols

Fig. 8a shows the drying curves of samples treated by hot air. It could be found that the hot air drying had the lowest drying efficiency. The total duration of hot air drying for carrot slices was 900 min to dry the moisture of carrot slices from 9.90 (kg/kg) to 0.11 kg/kg (d.b.). Besides, hot air drying might cause poor drying uniformity in multi-layer samples, and the same results are reported in a recent study (Zhou et al., 2018).

Fig. 8b shows the drying curves of samples treated by Comb-D 1 with the duration of 690 min. The drying efficiency of Comb-D 1 was improved by 23% than that of the hot air drying. Fig. 8c shows the drying curves of samples in each tray dried by Comb-D 2 with the duration of 675 min. Fig. 8d shows the drying curves of samples dried by Comb-D 3 with the duration of 630 min.

The difference among the drying curves of post individual hot air stage in the combined method was reduced (Fig. 8), especially comparing with the group dried by individual hot air. The same phenomenon has also been reported in a recent study (Zhou et al., 2018), because the RF field could convert weakly the bound water molecules to free water ones. According to this transformation in carrot slices in hot air assisted RF drying, the resistance of removing moisture from carrot slices in individual hot air processing was reduced. This result could also be found in Fig. 7, suggesting that RF energy could reduce the drying duration of carrot slices in multiple trays by keeping slices of each layer be dried uniformly.

The trends of drying rate in the Fig. 9 were also corresponding to the results in Fig. 7, the drying rates of individual hot air was lower than those of the combined method. The drying processing could be divided into three parts of period, corresponding to three stages of drying. The same results could also be found in Cui et al. (2004). The critical

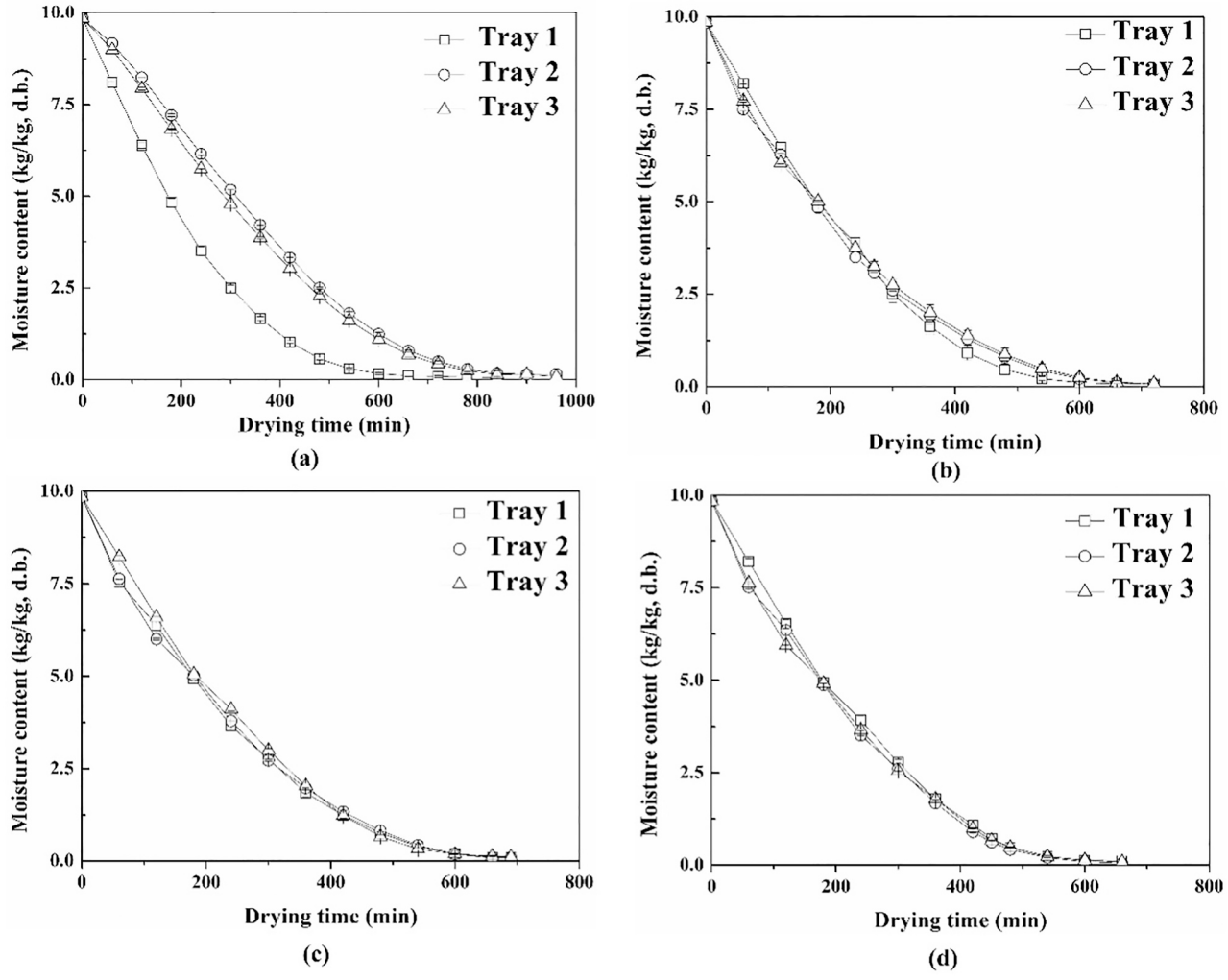

Fig. 8. Drying curves of the carrot slices with hot air drying (a), Comb-D 1 (b), Comb-D 2 (c) and Comb-D 3 (d).

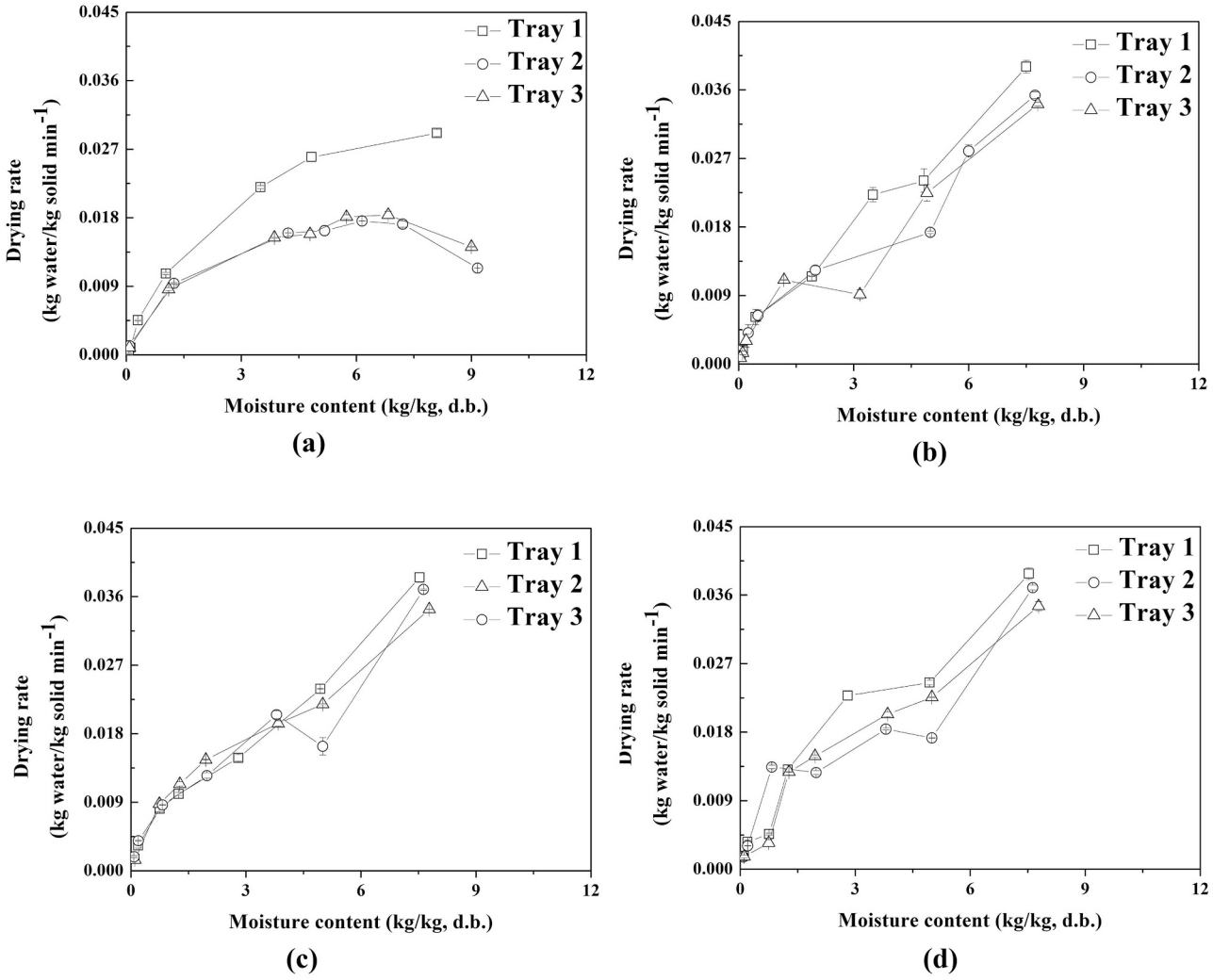

Fig. 9. Drying rates of carrot slices in three trays as a function of moisture content using hot air (a), Comb-D 1 (b), Comb-D 2 (c) and Comb-D 3 (d) drying methods.

Table 4
The average temperature and uniformity index (λ) of the slices at combined points in each layer using combined drying methods.

Combined point	Combined point 1	Combined point 2	Combined point 3
Average temperature (°C)			
Tray 1	42.19 ± 2.64	46.51 ± 1.77	56.91 ± 5.02
Tray 2	42.31 ± 1.64	46.49 ± 1.56	57.27 ± 8.03
Tray 3	41.52 ± 2.13	45.92 ± 1.57	56.54 ± 5.73
Uniformity index (λ)			
Tray 1	0.056 ± 0.022Aa#	0.057 ± 0.015Aa	0.123 ± 0.059Aa
Tray 2	0.045 ± 0.018Aa	0.051 ± 0.005Aa	0.225 ± 0.019Ba
Tray 3	0.049 ± 0.021Aa	0.052 ± 0.015Aa	0.153 ± 0.002Ba

Different lowercase and uppercase letters indicate that there is a significant difference ($P \leq 0.05$) in the heating uniformity index among trays and combined points, respectively.

moisture for the drying rate was about 1.0 (d.b.) or 0.5 (d.b.), the limit point to the second falling rate stage or final falling rate stage in drying. The drying rate of post individual hot air stage in the combined method was slower than the part of RF drying significantly. However, the advantage of high drying rate provided by RF energy was reduced in the final stage.

The average surface temperatures of the samples in each tray at the combined points were listed in Table 4. With the increased duration of hot air assisted RF drying, the average surface temperature of samples in the drying processing was increasing. Although the drying curves of combined methods showed that the duration for drying carrot slices was reduced by applying RF energy (Fig. 8), the heating uniformity decreased (Table 4). This increasing trend on the uniformity index (λ) of carrot slices at different combined points may be attributed to few high temperature points on carrot slices caused by the imbalance between the input heating energy and the latent heat to evaporate moisture in the final stage in hot air assisted RF drying, especially at the combined point 3 (Table 4).

To ensure the evaluation for drying methods by comparing the quality of products to be accurate, the slices in tray 2, with the highest temperature layer, were selected for further quality analysis based on the heating characteristics to evaluate the difference of heat-sensitive nutrients in products dried by different methods.

3.4. Effective diffusion and quality analysis of slices dried by different methods

The moisture effective diffusivity coefficient (D_{eff}) could reflect the difference of mass transfer in processing among different methods. The D_{eff} value for the protocol of Comb-D 3 was the highest in Table 5, showing the better mass transfer advantage of combined methods than individual hot air drying. To ensure the final products by taking

Table 5
The D_{eff}, color, and rehydration capacity of round carrot slices at final moisture content in tray 2 using different drying methods.

Treatments	D_{eff} (10^{-10} m^2/s)	L^*	a^*	b^*	ΔE	Rehydration ratio
Fresh	–	36.94 ± 1.06 A#	40.50 ± 0.82A	39.93 ± 0.27A	–	–
HAD	5.090	37.47 ± 0.46A#	34.51 ± 0.11B	35.16 ± 0.07ABC	8.04 ± 0.08A	2.53 ± 0.08C
Comb-D 1	5.726	37.31 ± 1.32A	35.03 ± 0.39B	36.46 ± 0.61 BCE	6.98 ± 0.13A	2.48 ± 0.07 BCE
Comb-D 2	6.360	39.51 ± 2.37A	34.03 ± 0.69AB	36.59 ± 1.10C	8.36 ± 0.26A	2.29 ± 0.02A
Comb-D 3	6.362	37.04 ± 1.26A	31.97 ± 1.66A	34.61 ± 0.03A	10.51 ± 1.47B	2.36 ± 0.03AB

Different uppercase letters indicate that the L^*, a^*, b^* values and the rehydration ratio of samples in tray 2 among different drying methods are significantly different at $P \leq 0.05$.

advantages both of mass transfer and quality attributes, the total carotenoid content is important to be investigated.

The quality attributes of products, which are selected to evaluate drying methods, are relative to heating characteristics, such as the residual content of the total carotenoid content and color attributes. The samples in tray 2 were used for quality analysis (Table 5). The quality results indicated that Comb-D 1 could improve the drying efficiency and avoid the serious loss of color in products. The ΔE of carrot slices treated by hot air drying was higher than that dried by Comb-D 1, which could be attributed to the long drying time using hot air, and the same results could be found in Alam et al. (2018) and Prieciņa and Kārkliņa (2018). The ΔE of slices dried by Comb-D 3 was larger than that of Comb-1, demonstrating that the high temperature and uneven heating caused by the imbalance energy input would reduce the color attributes of products.

The rehydration ratio of carrot slices dried by individual hot air, Comb-D 1, Comb-D 2 and Comb-D 3 were 2.53 ± 0.08, 2.48 ± 0.07, 2.29 ± 0.02, 2.36 ± 0.03, respectively (Table 5). This result may indicate that some irreversible physicochemical changes happened in the microstructure of carrot slices, and the same result could be found in Roknul et al. (2014). This could be attributed to the degradation of pectin content caused by the long duration and high temperature processing in carrot slices in drying, which could lead to collapse on microstructure, as studied in Nguyen, Mondor, and Ratti (2018) and Zhang et al. (2018).

The comparison of total carotenoid content of samples in tray 2 between the individual hot air and selected combined drying (Comb-D 1) was shown in Fig. 10. The total carotenoid content of samples dried by Comb-D 1 was significantly higher than that treated by individual hot air drying, Comb-D 2 and Comb-D 3 ($P < 0.05$). To take the advantages of mass transfer and high content of nutrients, the Comb-D 1 could be selected as an effective protocol to improve the drying efficiency and keep the total carotenoid content of carrot slices.

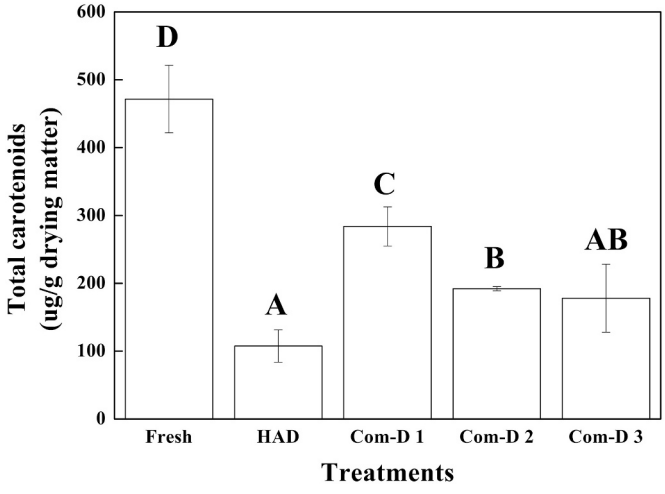

Fig. 10. Comparison of the total carotenoid content of carrot slices in tray 2 among fresh, hot air, Comb-D 1, Comb-D 2, and Comb-D 3 protocols (Different uppercase letters indicate that there is a significant difference ($P \leq 0.05$) in the total carotenoid content among different treatments).

4. Conclusion

This study focused on improving heating uniformity and drying efficiency without compromising the quality of product through layer rearrangements during hot air assisted RF drying of round carrot slices. The treatment protocol of a combined drying (Comb-D 1) was finally determined. Compared with the hot air drying, the selected combined protocol could effectively reduce the duration by 30%, and protect the color attributes of products effectively. Besides, the selected combined drying method could improve the retention of the total carotenoid content in products than the products processed by individual hot air drying significantly ($P \leq 0.05$). In future studies, determining the effect of combined methods on texture analysis is needed to reveal the mechanism of the heat and mass transfer in hot air assisted RF drying processing.

Author statement

CW conducted experiment, analyzed data, and wrote the first version of manuscript. XK assisted to conduct the experiments and product quality evaluation. XZ and RL assisted the experimental design and improved manuscript quality. SW is the PI of the project, guided the experimental design and revised manuscript.

Declaration of Competing Interest

The authors declare that they have no known competing financial interests or personal relationships that could have appeared to influence the work reported in this paper.

Acknowledgements

This research was conducted in the College of Mechanical and Electronic Engineering, Northwest A&F University, and supported by research grants from National Key Research and Development Program of China (2017YFD0400900) and Key Laboratory of Post-Harvest handling of fruits, Ministry of Agriculture (GPCH201703). The authors also appreciate Shuming Zhang in Nankai University for her technical assistance during the experiments.

References

Alam, M. R., Lyng, J. G., Frontuto, D., Marra, F., & Cinquanta, L. (2018). Effect of pulsed electric field pretreatment on drying kinetics, color, and texture of parsnip and carrot. *Journal of Food Science, 83*(8), 2159–2166.

Ando, Y., Okunishi, T., & Okadome, H. (2019). Influences of blanching and freezing pretreatments on moisture diffusivity and quality attributes of pumpkin slices during convective air-drying. *Food and Bioprocess Technology, 12*(11), 1821–1831.

Chen, Z. G., Guo, X. Y., & Wu, T. (2016). A novel dehydration technique for carrot slices implementing ultrasound and vacuum drying methods. *Ultrasonics Sonochemistry, 30*, 28–34.

Crank, J. (1975). *The mathematics of diffusion* (2nd ed.). London: Oxford University Press.
Cui, Z. W., Xu, S. Y., & Sun, D. W. (2004). Microwave-vacuum drying kinetics of carrot slices. *Journal of Food Engineering, 65*(2), 157–164.
Cui, Z. W., Xu, S. Y., Sun, D. W., & Chen, W. (2005). Temperature changes during microwave-vacuum drying of sliced carrots. *Drying Technology, 23*(5), 1057–1074.
Doymaz, I., & Aktas, C. (2018). Determination of drying and rehydration characteristics of eggplant slices. *Journal of the Faculty of Engineering and Architecture of Gazi University, 33*(3), 833–841.
FAOSTAT. (2018). Food and Agriculture Organization of the United States. http://www.fao.org/faostat/zh/?#data/QC/visualize. Access date: December, 2018.
Goula, A. M., & Adamopoulos, K. G. (2010). Kinetic models of β-carotene degradation during air drying of carrots. *Drying Technology, 28*(6), 752–761.
Guine, R. P. F., Brito, M. F. S., & Ribeiro, J. R. P. (2017). Evaluation of mass transfer properties in convective drying of kiwi and eggplant. *International Journal of Food Engineering, 13*(7), 20160257.
Hou, L., Huang, Z., Kou, X., & Wang, S. (2016). Computer simulation model development and validation of radio frequency heating for bulk chestnuts based on single particle approach. *Food and Bioproducts Processing, 100*, 372–381.
Hou, L. X., Liu, Q. Q., & Wang, S. J. (2019). Efficiency of industrial-scale radio frequency treatments to control Rhyzopertha dominica (Fabricius) in rough, brown, and milled rice. *Biosystems Engineering, 186*, 246–258.
Huang, Z., Zhang, B., Marra, F., & Wang, S. J. (2016). Computational modelling of the impact of polystyrene containers on radio frequency heating uniformity improvement for dried soybeans. *Innovative Food Science & Emerging Technologies, 33*, 365–380.
Jiao, Y., Tang, J., Wang, Y., & Koral, T. L. (2018). Radio-frequency applications for food processing and safety. *Annual Review of Food Science and Technology, 9*, 105–127.
Lau, W. K., Van Chuyen, H., & Vuong, Q. V. (2018). Physical properties, carotenoids and antioxidant capacity of carrot (Daucus carota L.) peel as influenced by different drying treatments. *International Journal of Food Engineering, 14*(3), 20170042.
Li, R., Kou, X. X., Cheng, T., Zheng, A. J., & Wang, S. J. (2017). Verification of radio frequency pasteurization process for in-shell almonds. *Journal of Food Engineering, 192*, 103–110.
Li, R., Kou, X. X., Hou, L. X., Ling, B., & Wang, S. J. (2018). Developing and validating radio frequency pasteurisation processes for almond kernels. *Biosystems Engineering, 169*, 217–225.
Li, Y., Li, F., Tang, J., Zhang, R., Wang, Y., Koral, T., & Jiao, Y. (2018). Radio frequency tempering uniformity investigation of frozen beef with various shapes and sizes. *Innovative Food Science & Emerging Technologies, 48*, 42–55.
Ling, B., Cheng, T., & Wang, S. J. (2020). Recent developments in applications of radio frequency heating for improving safety and quality of food grains and their products: A review. *Critical Reviews in Food Science and Nutrition, 60*(15), 2622–2642.
Maskan, M. (2001). Drying, shrinkage and rehydration characteristics of kiwifruits during hot air and microwave drying. *Journal of Food Engineering, 48*(2), 177–182.
Mbondo, N. N., Owino, W. O., Ambuko, J., & Sila, D. N. (2018). Effect of drying methods on the retention of bioactive compounds in African eggplant. *Food Science & Nutrition, 6*(4), 814–823.
Nguyen, T. K., Mondor, M., & Ratti, C. (2018). Shrinkage of cellular food during air drying. *Journal of Food Engineering, 230*, 8–17.
Prieciņa, L., & Kārkliņa, D. (2018). Influence of steam treatment and drying on carrots composition and concentration of phenolics, organic acids and carotenoids. *Proceedings of the Latvian Academy of Sciences. Section B. Natural, Exact, and Applied Sciences, 72*(2), 103–112.
Rawson, A., Tiwari, B., Tuohy, M., O'Donnell, C., & Brunton, N. (2011). Effect of ultrasound and blanching pretreatments on polyacetylene and carotenoid content of hot air and freeze dried carrot discs. *Ultrasonics Sonochemistry, 18*(5), 1172–1179.
Roknul, A. S., Zhang, M., Mujumdar, A. S., & Wang, Y. (2014). A comparative study of four drying methods on drying time and quality characteristics of stem lettuce slices (*Lactuca sativa L.*). *Drying Technology, 32*(6), 657–666.
Sezer, D. B., & Demirdoven, A. (2015). The effects of microwave blanching conditions on carrot slices: Optimization and comparison. *Journal of Food Processing and Preservation, 39*(6), 2188–2196.
Sutar, P. P., & Prasad, S. (2007). Modeling microwave vacuum drying kinetics and moisture diffusivity of carrot slices. *Drying Technology, 25*(10), 1695–1702.
Wang, S., Ikediala, J. N., Tang, J., Hansen, J. D., Mitcham, E., Mao, R., & Swanson, B. (2001). Radio frequency treatments to control codling moth in in-shell walnuts. *Postharvest Biology and Technology, 22*(1), 29–38.
Wang, S., Monzon, M., Johnson, J. A., Mitcham, E. J., & Tang, J. (2007). Industrial-scale radio frequency treatments for insect control in walnuts. *Postharvest Biology and Technology, 45*(2), 247–253.
Wang, S., Tiwari, G., Jiao, S., Johnson, J. A., & Tang, J. (2010). Developing postharvest disinfestation treatments for legumes using radio frequency energy. *Biosystems Engineering, 105*(3), 341–349.
Wang, Y. F., Wig, T. D., Tang, J., & Hallberg, L. M. (2003). Dielectric properties of foods relevant to RF and microwave pasteurization and sterilization. *Journal of Food Engineering, 57*(3), 257–268.
Wang, Y. Y., Zhang, L., Johnson, J., Gao, M. X., Tang, J., Powers, J. R., & Wang, S. J. (2014). Developing hot air-assisted radio frequency drying for in-shell macadamia nuts. *Food and Bioprocess Technology, 7*(1), 278–288.
Xu, W., Song, C., Li, Z., Song, F., Hu, S., Li, J., … Vijaya Raghavan, G. S. (2018). Temperature gradient control during microwave combined with hot air drying. *Biosystems Engineering, 169*, 175–187.
Zhang, B., Zheng, A., Zhou, L., Huang, Z., & Wang, S. (2016). Developing hot air-assisted radio frequency drying for in-shell walnuts. *Emirates Journal of Food and Agriculture, 28*(7), 459–467.
Zhang, H. J., Gong, C. T., Wang, X. F., Liao, M. J., Yue, J., & Jiao, S. S. (2019). Application of hot air-assisted radio frequency as second stage drying method for mango slices. *Journal of Food Process Engineering, 42*(2), Article e12974.
Zhang, M., Tang, J., Mujumdar, A. S., & Wang, S. (2006). Trends in microwave-related drying of fruits and vegetables. *Trends in Food Science & Technology, 17*(10), 524–534.
Zhang, Z., Wei, Q., Nie, M., Jiang, N., Liu, C., Liu, C., Li, D., & Xu, L. (2018). Microstructure and bioaccessibility of different carotenoid species as affected by hot air drying: Study on carrot, sweet potato, yellow bell pepper and broccoli. *LWT-Food Science and Nutrition, 96*, 357–363.
Zhou, L., Ling, B., Zheng, A., Zhang, B., & Wang, S. (2015). Developing radio frequency technology for postharvest insect control in milled rice. *Journal of Stored Products Research, 62*, 22–31.
Zhou, X., Gao, H., Mitcham, E. J., & Wang, S. (2017). Comparative analyses of three dehydration methods on drying characteristics and oil quality of in-shell walnuts. *Drying Technology, 36*(4), 477–490.
Zhou, X., Ramaswamy, H., Qu, Y., Xu, R., & Wang, S. (2019). Combined radio frequency-vacuum and hot air drying of kiwifruits: Effect on drying uniformity, energy efficiency and product quality. *Innovative Food Science and Emerging Technologies, 56*, 102182.
Zhou, X., & Wang, S. (2018). Recent developments in radio frequency drying of food and agricultural products: A review. *Drying Technology, 37*(3), 271–286.
Zhou, X., Xu, R., Zhang, B., Pei, S., Liu, Q., Ramaswamy, H. S., & Wang, S. (2018). Radio frequency-vacuum drying of kiwifruits: Kinetics, uniformity, and product quality. *Food and Bioprocess Technology, 11*(11), 2094–2109.